R. & M. No. 3114
(19,630)
A.R.C. Technical Report

MINISTRY OF SUPPLY

AERONAUTICAL RESEARCH COUNCIL
REPORTS AND MEMORANDA

Experimental Observation of Vortices in Wing-Body Junctions

By

A. STANBROOK

LONDON: HER MAJESTY'S STATIONERY OFFICE
1959
EIGHT SHILLINGS NET

Experimental Observation of Vortices in Wing-Body Junctions

By

A. STANBROOK

COMMUNICATED BY THE DIRECTOR-GENERAL OF SCIENTIFIC RESEARCH (AIR), MINISTRY OF SUPPLY

Reports and Memoranda No. 3114*

March, 1957

Summary.—Tests have been made on various wing-body combinations to investigate the nature of the flow in the junction. It was found that vortices are formed due to separation of the boundary layer on the body in the flow towards the wing. The free edge of the resulting vortex sheet rolls up to form the vortex which then trails downstream around the wing. As incidence is increased the vortex on the suction side of the wing moves towards the wing and the vortex on the pressure side moves away from the wing.

The vortices are present with both swept and unswept rounded leading edges at subsonic and supersonic speeds but were not found with sharp leading edges at zero incidence.

1. *Introduction.*—In the investigations reported in Ref. 1 measurements were made of the pressure distribution on a combination of a body and a delta wing at supersonic speeds. Certain characteristics of the pressure distribution on the body suggested the presence of vortices in the neighbourhood of the junction of the wing and body. This has been confirmed by further tests on the same model, and the effects of incidence and Reynolds number on the strength and position of the vortices have been studied. Other models have been used to investigate the effects of leading-edge shape and sweep at both subsonic and supersonic speeds.

Vortices of the type investigated here have been observed before. For instance, similar vortices can cause the spread of turbulence from isolated surface excrescences in a laminar boundary layer[2], while others have been found in cascades of aerofoils (*see*, for instance, Refs. 3 and 4) where they are associated with serious loss of pressure ratio. They are also produced freely by the natural wind and may be observed to the windward side of isolated hills and houses. In fact, the indentations in deposited snow to the windward side of houses, trees, etc., are caused by the scouring action of the vortices.

The investigations described here were carried out during the period 1952 to 1954. Since then the vortices have been observed elsewhere (*see*, for instance, Ref. 5). The only previous report of their effects on the flow around the wing roots of aircraft appears to be that of Zwaanewald[6].

Since the present interpretation of these results was obtained, Maskell[7] has described possible types of flow pattern near a separation line in three dimensions in general terms, and has included the type of flow chiefly considered here as one of his examples: reference has been made to his nomenclature where possible.

* R.A.E. Report Aero. 2589, received 5th November, 1957.

Throughout the report the term ' vortex ' is used loosely to describe a more-or-less rolled-up vortex sheet with a core of low total head and low static pressure.

2. *Tests on the Wing-Body Combinations.*—2.1. *Delta Wing.*—Fig. 1 shows the general arrangement of the delta wing-body combination. It consists of a 60-deg delta wing with a 6 per cent thick RAE 101 section on a cylindrical body to which may be attached one of three conical noses of 15-deg apex semi-angle with different cylindrical lengths downstream of the shoulder or a slightly blunted ogive 3·6 diameters long. Further details may be obtained from Ref. 1. The pressure distribution on this model was measured at a Mach number of 1·61 in the 3 ft × 3 ft Supersonic Wind Tunnel at the Royal Aircraft Establishment, Bedford. For the majority of the pressure-plotting tests the total pressure was 38 in. of mercury, giving a Reynolds number of $0{\cdot}47 \times 10^6$ per in. ($3{\cdot}5 \times 10^6$ based on root chord). At one stage, however, the model was tested over a range of total pressures giving Reynolds numbers from $0{\cdot}13 \times 10^6$ to $0{\cdot}47 \times 10^6$ per in. A transition wire, 0·004 in. in diameter, was attached round the nose of the body approximately 2·5 in. from the apex, except where otherwise stated. The effectiveness of this wire in causing transition of the boundary layer was checked by the sublimation technique using azobenzene.

The pressure distributions along the body at incidences of 0, 4 and 10 deg are shown in Figs. 2, 3 and 4 respectively. The presence of vortices was originally suggested by the suction peak approximately 3 in. from the wing-root leading edge in the pressure distribution along the line 30 deg below the plane of the wing at 10-deg incidence (Fig. 4). The pressure distribution would be expected to be fairly level upstream of the wing with a sharp increase in pressure through the leading-edge shock wave followed by a gradual decrease in pressure as the flow accelerates beneath the wing and a rapid decrease through the expansion around the trailing edge. There are also indications of superimposed local reductions in pressure (to a smaller degree) at 0 and 4-deg incidence. The hump in the pressure distribution along the 60-deg line on the suction side at 10-deg incidence is thought to be caused by the proximity of the vortex formed by the cross-flow about the body.

The regions around the body in which the presence of vortices was suspected were traversed with the double row of pitot-pressure probes shown in Figs. 5 and 6. These pitot probes were always aligned with the body axis. Contours of p_m/H, where p_m is the measured pitot pressure and H is the total pressure in the free stream, are shown in Figs. 7 and 8 for stations at 0·57 and 0·87 root chord. Traverses with the pitot-pressure probes were also made around the body alone at 9 in. and 14 in. from the cone shoulder (equivalent to 0·20 and 0·87 root chord respectively). The contours of p_m/H obtained at 10-deg incidence are shown in Fig. 9. The value of p_m/H in the free stream is 0·892 due to the loss of total pressure through the bow shock wave of the pitot tubes themselves. It should be noted here that these pitot-pressure traverses were intended to be of a qualitative nature only. Because of the wide spacing of the tubes it is not possible to obtain reliable estimates of the relative strengths of the vortices from these results alone.

The pitot-pressure contours obtained around the wing-body combination (Figs. 7 and 8) show two regions of reduced pitot pressure outside the boundary layer, one above the wing and the other below it. By comparison with the contours obtained around the body alone (Fig. 9) the low-pressure region detected on the suction side of the model has been identified as the core of a vortex formed by the cross-flow about the body. On the other hand, the low-pressure region detected on the pressure side of the model has no counterpart in the body-alone case and must be due, in some way, to the wing.

The oil-flow technique was then used to give a visual indication of the streamlines at the surface (the ' limiting streamlines ' of Ref. 7). For this a very thick oil (Shell Nassa 87) was used as carrier, titanium oxide as colouring matter and oleic acid as an anti-coagulant. The mixture was brush-painted on to the model as thinly as possible. About 20 minutes were occupied in starting the tunnel at low pressure and bringing the pressure up to the operating value. During the following 10 to 15 minutes the oil flowed slowly into a definite pattern, which was photographed

through the schlieren windows with the tunnel still running. (The reason for the use of a thick oil rather than the thin oil of the low-speed tunnel 'paraffin and lampblack' technique was the need to limit the movement of the mixture during the tunnel starting period. A disadvantage of the use of thick oil is that no final set pattern is obtained, the whole mixture moves slowly downstream and blows off the tail of the model. A photograph taken after stopping the tunnel is inevitably distorted if the model has first to be brought to zero incidence and the stagnation pressure reduced. Thick oil is also used in water tunnels where, even at low speeds, the skin friction is higher than in high-speed wind tunnels. The application of this technique in the 3 ft tunnel has been improved considerably since these tests were made.)

Photographs obtained in this way are shown in Figs. 2, 3 and 4 for incidences of 0, 4 and 10 deg respectively*. Schlieren photographs of the overall flow pattern were also obtained at these incidences. It was felt, however, that these contain extraneous details which tend to confuse the discussion of the present subject and the photographs are not presented. The positions of the relevant shock and expansion waves have been obtained from these photographs and are indicated on the oil-flow photographs. In Fig. 2, at $\alpha = 0$, the oil lines on the body pass well clear of the wing and there is a region adjacent to each surface of the wing which has been swept almost clear of oil. This region reaches its maximum width near mid-chord, after which it contracts towards the trailing edge. Downstream of the trailing edge it diverges again slightly. The few streaks of oil remaining in the region near the trailing edge undergo a sudden change in direction where, from the schlieren photographs, the trailing-edge shock wave appears to be. At 4-deg incidence (Fig. 3) the region cleared of oil has become wider on the pressure side but has decreased in width on the suction side where it appears to end at about mid-chord. At 10-deg incidence (Fig. 4) this process has continued, so that the cleared region on the suction side is almost non-existent. In this photograph enough oil remains in the highly scoured region on the pressure side to show that this region may be divided into three distinct regions. One is adjacent to the wing downstream of the quarter-chord point and here the flow direction is approximately parallel to the wing surface. In the other two regions the oil flows away from the wing and downstream. There is a clearly marked outer limit to the inner of these two regions while the outer one is only clearly defined near the leading edge of the wing where it appears to originate at the foot of the leading-edge shock wave. Again, in both Fig. 3 and Fig. 4 there is a sharp change in direction of the oil lines at the upper-surface trailing-edge shock wave. Downstream of the trailing edge at 10-deg incidence the oil lines from the pressure side of the wing show a marked upward trend towards a line approximately one third of a body radius above the wing plane.

The sweeping away of oil from the wing root would be consistent with the presence of a vortex wrapped round the leading edge, having a rotation which is always away from the wing at the body surface. This concept is supported by the presence of suction peaks in the static-pressure distribution and regions of low pitot pressure in the pitot-pressure distributions observed with the model at incidence. It appears from the oil-flow patterns that at zero incidence the vortex lies fairly close to the wing. In this case it would not be detected by the pitot-pressure traverse and would not cross the line of pressure holes 30 deg from the plane of the wing. The observed effect on the pressure distribution along this line is slight and can only be recognised by comparison with the two non-zero incidence cases.

The variation in size of the regions scoured by the vortices in the oil-flow patterns suggest that at incidence the vortex on the pressure side of the wing moves away from the wing so that it crosses the line of pressure holes 30 deg from the plane of the wing and moves into the region traversed by the pitot-pressure probes. Its presence is indicated by the marked suction peak on the line 30 deg from the plane of the wing approximately 3 in. from the wing-root leading edge

* In these photographs the root section has been blanked in to avoid confusion. The short, light bars approximately normal to the wing surface across the wing chord are the slots in which the pressure leads run to the inside of the model. These are filled with solder and finished flush with the surface.

(Figs. 3 and 4). The vortex appears to recross this line further downstream (approximately 8 in. and 9·5 in. downstream of the wing-root leading edge for $\alpha = 4$ deg and 10 deg respectively) with a less pronounced suction peak. The reduction in the suction peak indicates that the vortex has either decreased in strength or moved away from the body surface in the interval. The region of low pitot pressure on the pressure side of the wing in Figs. 7 and 8 is caused by the core of the vortex.

Again, from the oil-flow patterns it appears that at incidence the vortex on the suction side of the wing moves closer to the wing. As a result, it no longer affects the measured static-pressure distribution on the body. As the incidence is increased this vortex probably moves out over the wing and it could be expected to influence the static-pressure distribution there. However, due to the paucity of the pressure-measuring points on the wing, particularly along the spanwise direction, it was not possible to detect this. Also, observations of oil flow on the wing surface do not show the presence of this vortex very clearly since other details of the flow on the wing confuse the picture. An attempt was made to observe the vortices by the ' vapour screen ' method but no conclusive result was obtained, probably because the cores were too small and the reflections from the body too bright.

An indication of the effect of the Reynolds number and the condition of the boundary layer on the position of the vortex was obtained from further pressure measurements. Pressure distributions along the line 30 deg from the plane of the wing were measured at 10 deg incidence with various nose lengths and at various total pressures.

The effect of Reynolds number on the pressure distribution along this line for the wing-body combination with nose C (Fig. 1) is shown in Fig. 10 together with oil-flow patterns on the side of the body at two Reynolds numbers. The oil-flow patterns show no noticeable difference in the surface streamlines at the two Reynolds numbers but the pressure distributions show that the suction peak caused by the vortex moves downstream slightly as the Reynolds number is decreased. This suggests that the vortex moves closer to the wing. The magnitude of the suction peak is also reduced. At the lowest Reynolds number tested ($0{\cdot}13 \times 10^6$ per in.) a second suction peak is noticed approximately 5·5 in. downstream of the root-chord leading edge. This is the position where the vortex crosses the line again and confirms the suggestion that the vortex is closer to the wing.

The effect of changing the nose length and shape on the pressure distribution at constant Reynolds number per inch is shown in Fig. 11a. To make some allowance for the change in the pressure distribution due to the body itself Fig. 11b shows the difference between the pressure distributions on the bodies of the wing-body combination and those on the corresponding bodies alone. It will be seen that reducing the nose length by one diameter (replacing nose C by nose B (*see* Fig. 1)) appears to move the suction peak downstream slightly and to reduce its magnitude but an additional reduction by one diameter (to nose A) appears to have no further effect. In Fig. 11a the pressure distribution between 4 and 7 in. downstream of the leading edge could be interpreted as indicating that the vortex crosses the line again and the agreement between the curves for noses A and B in Fig. 11b may be purely coincidental. However, on the basis of the results presented in Fig. 10, it seems unlikely that the vortex would cross the 30-deg line at this point without a corresponding shift of the forward suction peak. The pressure distribution due to the wing on the ogival-nosed body is almost exactly the same as with nose B, as could be expected from their similarity of length (*see* Fig. 1).

In the first of these two tests the estimated boundary-layer thickness increases as the Reynolds number is reduced. In the second test a decrease in nose length reduces both the boundary-layer thickness and the Reynolds number at the wing-root leading edge. It would appear, therefore, that varying the thickness of the body boundary layer has relatively little effect, in itself, on the position and strength of the vortices, but that a reduction in Reynolds number at the wing-root leading edge causes the vortex to move closer to the wing. At the same time the magnitude of the suction peak caused by the vortex is reduced, indicating that the vortex is either weaker or

further from the surface of the body. The movement is, however, only slight and it is merely because the vortex crosses the line of pressure holes at such an oblique angle that the movement was detected. The two oil-flow pictures in Fig. 10 do not show any noticeable displacement.

Fig. 11a also shows the effect of removing the transition wire from the nose of the body. Transition then occurred somewhere in the interaction region of the wing leading-edge shock wave and the body boundary layer; this was in fact checked by the sublimation technique using azobenzene. In the absence of the wing transition occurs downstream of this region. The vortex appears to be weaker and closer to the wing with free transition.

It was remarked earlier that there are abrupt changes in direction of the oil lines at the shock waves from the leading and trailing edges of the wing. This change in flow direction within the boundary layer is, in fact, greater than in the external flow, since the increased pressure acts on slower-moving air than outside the boundary layer. The marked upward trend of the oil lines downstream of the trailing edge in Figs. 4 and 10 is caused by a similar process acting within the expansion fan on the lower surface at the trailing edge.

The flow of oil on the model was also observed at a Mach number of 0·70 to determine whether the effects at subsonic and supersonic speeds are qualitatively similar. This was found to be so. The photographs obtained are shown in Fig. 12. They are again characterized by a region, adjacent to the wing, cleared of oil. The width of the region is less than at supersonic speed, particularly close to the trailing edge. At incidence the size of the cleared region is again decreased on the suction side and increased on the pressure side, although the rate of change of size of the regions with incidence is less and there is still a region at moderate size on the suction side at 10-deg incidence. The main difference is due to the concentration of the pressure field of the wing at supersonic speeds into the region between the shock and expansion waves from the leading and trailing edges and particularly to the abrupt increases and decreases in pressure through these waves. At subsonic speeds pressure changes are more gradual and abrupt changes in directions of the oil lines are not observed.

2.2. *Rectangular Wings.*—Further visualization tests were made on two wing-body combinations with the plan-form shown in Fig. 13. One wing had a 6 per cent thick RAE 101 section while the other wing had a wedge section with 10-deg total angle and a blunt base perpendicular to the chord. These tests were made at Mach numbers of 0·70 and 1·61 at total pressures of 36 and 31 in. of mercury respectively, giving a Reynolds number of $0{\cdot}38 \times 10^6$ per in. ($1{\cdot}5 \times 10^6$ based on the chord). A transition wire, 0·004 in. in diameter, was attached round the nose of the body approximately 2·5 in. from the apex.

The photographs* obtained at $M = 1{\cdot}61$ are shown in Fig. 14 for the RAE-101-section wing and in Fig. 15 for the wedge-section wing. The position of the shock and expansion waves are again indicated. Pressure measurements were also made at this Mach number and the pressure distribution along the lines 30 deg from the plane of the wing are shown in coefficient form in Fig. 16 for the RAE-101-section wing at 8-deg incidence and for the wedge-section wing at 10-deg incidence. The curves have been drawn using the schlieren photographs and oil-flow patterns to indicate the exact position of the individual pressure changes.

The flow patterns on the body with the RAE-101-section rectangular wing (Fig. 14) are similar to those obtained with the delta wing, but the width of the region of outward scouring is much greater, particularly when considered relative to the root chord. Near the leading edge of the wing at zero incidence the oil streamlines on the body are deflected through about 70 deg away from the wing at the approximate shock position. There is no clear indication of a vortex trailing downstream. At 4 deg and 8 deg the oil-flow lines suggest that separation occurs in the neighbourhood of the leading edge, particularly below the wing plane. Between this separation line and the pressure surface of the wing the surface pattern appears to be divided into at least three regions. The one adjacent to the wing contains oil lines which are approximately parallel to the wing surface. In the other two regions the oil flows away from the wing and downstream

* The end view of the wing has again been blanked in, but in these cases the effect of perspective is such that it has sometimes been necessary to indicate the position of the root by broken lines.

and it would appear that two separate vortices may be present. As with the delta wing, the shape of the highly scoured region above the wing suggests that the vortex curves round the leading edge and is deflected down on to the wing at a point which moves forward with increasing incidence. At the trailing-edge upper-surface shock wave the oil lines are again deflected through a large angle and a further vortex appears to be formed just downstream of this shock wave at $\alpha = 8$ deg. The pressure distributions in Fig. 16a show a single suction peak immediately downstream of the leading-edge shock wave on the pressure side of the wing, indicating the presence of a vortex. Further downstream the flow accelerates over the wing until the expansion fan from the trailing edge is reached, where there is a rapid decrease in pressure. On the suction side of the wing the flow undergoes a slight compression through the (detached) shock wave followed by an expansion around the leading edge. The flow continues to accelerate past the wing until the trailing-edge shock wave is reached, when the pressure rises rapidly.

At zero incidence on the body with the wedge-section rectangular wing (Fig. 15) there is a fairly large triangular region, with its apex at the leading edge, which has been almost cleared of oil. The few oil traces remaining in this region are not strongly suggestive of the presence of a vortex. At 4-deg incidence there is still no sign of a vortex on the suction side of the wing. On the pressure side the oil lines are turned through a sharp angle at the approximate position of the leading-edge shock wave and a little downstream of this position they form the envelope of the scoured region adjacent to the wing. Within this region the flow is predominantly away from the wing, again suggesting the presence of a vortex. At 10-deg incidence the leading-edge shock wave is detached from the wing and the oil-flow pattern definitely suggests that the boundary layer has separated at the base of this shock wave on the pressure side of the wing. Immediately downstream of this separation line the oil-flow lines are not very distinct and it would appear that there is a local separation bubble. Closer to the wing-body junction there is an outflow away from the wing which has already been seen to be characteristic of the vortex. In the region adjacent to the wing the streamlines are nearly straight and are very slightly inclined towards the wing surface. The boundary layer appears, from the schlieren observations, to separate at the bottom of the body where the shock waves from the two wings meet. The accumulation of oil just above the plane of the wing upstream of the leading-edge shock wave is due to the vortex in the crossflow about the body. Immediately downstream of the leading edge this oil flows down towards the wing. The cleared region adjacent to the suction surface of the wing is so small that it is not clear whether a vortex is present or not. In each of the three photographs in Fig. 15 the flow appears to separate at the base of the shock waves from the wake just downstream of the blunt trailing edge and there are regions of outward sweep of the oil which again suggests the presence of vortices.

In the pressure distribution in Fig. 16b a suction peak immediately downstream of the leading-edge shock wave, approximately one inch downstream of the leading edge, indicates the presence of the vortex on the pressure side of the wing.

Further downstream the flow expands around the blunt trailing edge until it reaches the shock wave from the point where the wakes from the upper and lower surfaces combine. On the suction side of the wing the flow expands over the leading edge. It then passes through a region of gradual recompression where the effect of the higher-pressure regions further out across the wing (due to the decrease in the body upwash at greater distances from the body) is felt. The flow then expands around the blunt trailing edge until it reaches the shock wave from the wake. Downstream of this shock wave the vortex which originates at its base causes a slight reduction in the local pressures.

Fig. 17 shows a selection of the oil-flow patterns obtained with these two wing-body combinations at $M = 0{\cdot}70$. The top photograph shows the pattern obtained with the wedge-section wing at zero incidence. It will be seen that there is no region adjacent to the wing which is cleared of oil and, hence, it appears that there is no vortex produced in this case. At incidence with this wing there are signs of the presence of a vortex on the pressure side of the wing but the pattern was complicated by the presence of a leading-edge separation on the suction side of the wing.

The remaining two photographs in Fig. 17 show the flow with the RAE-101-section wing at $M = 0{\cdot}70$ at zero incidence and at 8 deg. At zero incidence there is only a very small region adjacent to the wing which is cleared of oil. This region again contracts towards the trailing edge and then diverges. At 8-deg incidence the width of the region cleared of oil on the pressure side has increased and there are some traces of an outflow of oil within this region. On the suction side of the wing the flow outside the boundary layer has separated from the wing at the leading edge and there are, consequently, no definite indications of the presence of the vortex there.

2.3. *Swept Wing.*—An additional example of the presence of these vortices (suggesting the presence of more than one vortex either side of the wing) was obtained, incidentally, during a series of tests at a Mach number of $1{\cdot}81$ on the swept wing and body combination shown in Fig. 18. The wing and body were sprayed with azobenzene for observations, by the sublimation technique, of boundary-layer transition on the wing at zero incidence. Streaks suggesting the presence of five near-streamwise vortices were seen originating at the intersection of the wing shock wave and the body (*see* Fig. 19).

3. *Interpretation and Discussion of the Experimental Results.*—It is believed that the vortices investigated here originate in separations of the fuselage boundary layer in the flow towards the wing.

The mechanism of their formation may perhaps be best understood by referring back to the two-dimensional flow up a step and by tracing the connection between this and the three-dimensional flow past a wing root.

Lighthill[8] has studied, analytically, the type of two-dimensional flow that occurs at a step formed by two flat plates, at right angles, placed with one plate parallel to the oncoming stream (Fig. 20). Separation occurs at some point, B, downstream of the leading edge, A, of the plate. Beyond B the external flow follows the free streamline BCE (which bounds regions of air very nearly at constant pressure, BCD, CDE). The vortex sheet BC is assisted in remaining stable by the proximity of the solid boundary BDC. Lighthill found the position of separation, B, for various ratios of the lengths of the two plates (AD/DC) for both laminar and turbulent boundary layers.

Now consider what happens when the plate CD is of limited spanwise extent. If the span is large then near its centre the flow pattern will be very similar to the two-dimensional pattern with the vortex sheet from the plate AD to the edge C enclosing a bubble, BCD. At the ends of the span the vortex sheet will leave the plate CD and turn downstream. The stabilising influence of the plate will be lost and the free edge of the vortex sheet will roll up. This rolling-up will, in fact, begin further upstream around the forward face of the plate CD.

If the span of the plate CD is small a flow pattern of the two-dimensional type may not occur at all. The vortex sheet originating at the separation point B will not reach the plate CD but will roll up somewhat upstream and curve around the ends of the plate. The rolled-up portion of the vortex sheet will draw high-energy air into the region beneath the vortex sheet producing a flow on the surface, from the plate towards the original separation line (Fig. 21). This flow will tend to separate as it passes beneath the vortex. The vortex sheet resulting from this ' secondary ' separation may either roll up to form a secondary vortex or, as shown in Fig. 21, combine with the original vortex sheet to bound a bubble.

The extension of this model of the flow to the flow around a wing root within the boundary layer of a wall or a fuselage is straightforward (Fig. 22). The boundary layer (on the wall or fuselage) separates upstream of the leading edge of the wing and the external flow then follows the free vortex sheet to the point where it rolls up. Some of the external flow is then drawn down on to the surface at an attachment line lying either on the wing or between the wing and the original separation line and flows away from the wing surface towards the underside of the vortex sheet. The fluid may separate as it passes beneath the vortex. The behaviour of this secondary

separation will depend on a number of factors which are not yet understood; in general, the resulting vortex sheet will either roll up to form a secondary vortex or will combine with the original vortex sheet to bound a bubble. The original separation persists downstream of the leading-edge region and the vortex sheet may split and roll up to form more than one vortex.

Fig. 23 shows an interpretation of Fig. 15c based on this general description of the phenomenon. Separation of the body boundary layer occurs slightly upstream of the (detached) leading-edge shock wave (section AA). The resultant vortex sheet rolls up between the shock wave and the wing and induces a flow down beneath the vortex sheet itself, the fluid flowing forwards away from an attachment line very close to the wing-body junction towards the separation line. This is not reached, however, since the flow separates from the surface as it passes beneath the vortex.

Further downstream, away from the shock wave, the vortex becomes roughly parallel with the wing surface. The induced flow beneath the vortex has now a downstream component but it is still predominantly away from the wing surface and it continues to separate before it can reach the outer separation line. The exact behaviour of the fluid in the region between the two separations is not known with any certainty but it is thought that the vortex sheet may be ' torn ' into two segments, each of which rolls up to form a vortex (section BB)*.

The boundary layer separates along the entire length of the wing leading-edge shock wave on the pressure side of the wing. On the bottom of the body, where the shocks from the two wings intersect, the boundary layer was seen to separate in the schlieren photographs; the probable pattern downstream of this point is illustrated in section CC.

The effects of Mach number on the occurrence of separation are mainly due to the different types of basic flow pattern at subsonic and supersonic speeds. Thus at subsonic speeds the occurrence of separation can be influenced by the whole of the flow field around the wing. As an indication of the initial separation position, it is possible, using available three-dimensional boundary-layer theory[10], to calculate the flow of a laminar boundary layer up to the stage at which an envelope of the surface streamlines is formed. This appears, from work such as that of Maskell[7], to be a necessary condition for boundary-layer separation. At supersonic speeds the adverse pressure gradient upstream of the wings is concentrated within the leading-edge shock wave and the occurrence, or otherwise, of separation will probably depend upon the strength of this shock wave (as in two-dimensional flow). This point is amply illustrated by Fig. 15. At zero incidence the shock wave is not strong enough to cause separation anywhere along its length and the surface streamlines are merely turned through a greater angle than the streamline outside the boundary layer by the transverse pressure gradient. At 4-deg incidence the shock wave causes the boundary layer to separate at the wing-body junction but further away from the wing (where the shock strength is reduced by the transverse curvature of the body) separation does not occur. At 10-deg incidence separation occurs along the entire length of the shock wave on the pressure side of the wing. From a general point of view, the effects of both Mach number and incidence may be associated with the general alteration of the flow pattern near the leading edge; at supersonic speeds the significant alteration appears to be the variation in lateral extent of the segment of the leading-edge shock wave which is strong enough to cause separation.

The variation of Reynolds number and of boundary-layer thickness which was achieved in the tests covered only a very limited range and consequently little can be said about their effects on the formation, position, and strength of the vortices. In particular, nothing is known of the importance of the overall effects in the range of Reynolds number corresponding to full-scale aircraft flight.

* The formation of more than one vortex appears to be a fairly frequent occurrence at the higher incidences (Figs. 4, 14b, 14c and 15c) and there is some evidence for believing that it occurs at zero incidence (Fig. 19), although this latter case may be exceptional. Although none of the subsonic patterns obtained in the present investigation showed this feature, flow patterns have been observed in a low-speed tunnel at incidences between 12 deg and 20 deg which do show the presence of two vortices on the pressure side of a wing. Gregory and Walker[2] have also observed multiple vortices around the root of a circular cylinder in a laminar boundary layer at low speeds. In a related case, Sutton[9] has observed multiple vortices on a wing with leading-edge separation and has also suggested that the separated vortex sheet ' tears ' and rolls up in sections.

However, the more obvious of the possible overall effects of the presence of the vortices are worth noting. First, they are thought to be associated with the loss of lift known to occur within the boundary layer of the wall, or fuselage, on which the wing is mounted[11,12]. (At the very least, it may be said that previous attempts to calculate the effect of the wall boundary layer on the lift in the root region have been based on an incomplete physical picture of the flow.) Then, since the presence of these wing-root vortices involves a continuous shedding of vorticity from the body boundary layer into the stream, it is probable that they produce a form of induced drag, even at zero incidence. Further, if present in the vicinity of tail surfaces, they could induce forces with destabilizing effects, particularly in asymmetric conditions. Also, the redistribution of low-energy and high-energy air, from the body boundary layer and the external flow, associated with the vortices could have large effects on intakes downstream of the wing. As was stated earlier, because of the very limited nature of the existing data, it is difficult to make any general assessment of the overall importance of these effects.

It is natural to enquire whether aerofoil sections could be designed to prevent the occurrence, or limit the extent, of separation. This has been done by Loos[13] and Hawthorne[14] for low-speed flow, using secondary-flow theory. Secondary-flow theory does not actually predict separations of the type considered here but predicts infinite values of the vorticity at some points inside the region where the flow would be separated. Loos has shown that these infinities are dependent on the angle that the flow has to turn through at the stagnation point. If this angle is less than 90 deg then the vorticity is finite. In the flow about the wedge wing at zero incidence the flow only has to turn through 5 deg and Fig. 17a, for $M = 0{\cdot}70$, shows neither separation nor vortex. Loos also considered the flow around a circular arc, without a stagnation point, and found finite vorticity. Hawthorne developed a method for designing sections which should produce low secondary vorticity and used it to design a bi-cusped profile. He then demonstrated the improvement in a water channel by comparing the scouring actions of the flow around this profile and the flow around an elliptic section of the same thickness/chord ratio. It should be possible (although laborious) to check whether separation would or would not occur with these sections by the application of three-dimensional boundary-layer theory. Unfortunately such a theory does not exist for turbulent boundary layers at present.

It is as well to note that these vortices will be (and always have been) present in the flow around all round-nosed or bluff protuberances on aircraft (such as canopies, airbrakes, etc., as well as the main lifting and stabilizing surfaces), and that a knowledge of their presence and behaviour will assist in the interpretation of surface oil-flow patterns.

4. *Conclusions.*—Tests have been made on various wing-body combinations to investigate the nature of the flow in the junction. It was found that vortices are formed due to separation of the boundary layer on the body in the flow towards the wing. The free edge of the resulting vortex sheet rolls up to form the vortex, which then trails downstream around the wing. As incidence is increased the vortex on the suction side of the wing moves towards the wing and the vortex on the pressure side moves away from the wing.

The vortices are present with both swept and unswept rounded leading edges at subsonic and supersonic speeds but were not found with sharp leading edges at zero incidence.

REFERENCES

No.	Author	Title, etc.
1	A. Stanbrook and E. P. Sutton	Experimental pressure distributions on a cylindrical-body and delta-wing combination at Mach numbers of 1·42 and 1·61. Preliminary data. R.A.E. Tech. Note Aero. 2250. July, 1953.
2	N. Gregory and W. S. Walker	The effect on transition of isolated surface excrescences in the boundary layers. R. & M. 2779. October, 1950.
3	A. D. S. Carter and E. M. Cohen	Preliminary investigation into the three-dimensional flow through a cascade of aerofoils. R. & M. 2339. February, 1946.
4	A. G. Hansen, Z. Henzig and R. Costello	A visualization study of secondary flows in cascades. N.A.C.A. Report 1163. 1954.
5	J. R. Busing and G. M. Lilley	A preliminary investigation of the flow over a particular wing-body combination at Mach number 2. College of Aeronautics Note No. 24. April, 1955.
6	J. Zwaanewald	Orienterend onderzoek van interferentie-verschijnselen afkomstig van grenslaag-effecten aan de wortel van een aan een wand (romp) bevestigde vleugel. Stromingsonderzoekdoor. N.L.L. Report A. 1265. November, 1951.
7	E. C. Maskell	Flow separation in three dimensions. R.A.E. Report Aero. 2565. A.R.C. 18,063. November, 1955.
8	M. J. Lighthill	On boundary layers and upstream influence. 1—A comparison between subsonic and supersonic flows. *Proc. Roy. Soc.* Series A. Vol. 217. A. 1130. pp. 344 to 357. May, 1953.
9	E. P. Sutton	Some observations of the flow over a delta-winged model with 55-deg leading-edge sweep, at Mach numbers between 0·4 and 1·8. R.A.E. Tech. Note Aero. 2430. A.R.C. 18,072. November, 1955.
10	L. C. Squire	An approximate method for boundary layers on general bodies. Thesis. Bristol University. 1956.
11	W. L. Cowley and G. A. McMillan	Pressure exploration over an aerofoil that completely spans a wind tunnel. R. & M. 1597. October, 1933.
12	R. A. Mendelsohn and J. F. Polhamus	Effect of the tunnel-wall boundary layer on test results of a wing protruding from a tunnel wall. N.A.C.A. Tech. Note 1244. April, 1947.
13	H. G. Loos	Enige beschouwingen over de grenslaaginterferentie bij de aansluiting van een draagvlak en een wand. N.L.L. Report A. 1282. February, 1952.
14	W. R. Hawthorne	The secondary flow about struts and aerofoils. *J. Ae. Sci.* Vol. 21. No. 9. pp. 588 to 608. September, 1954. A.R.C. 16,238. October, 1953.

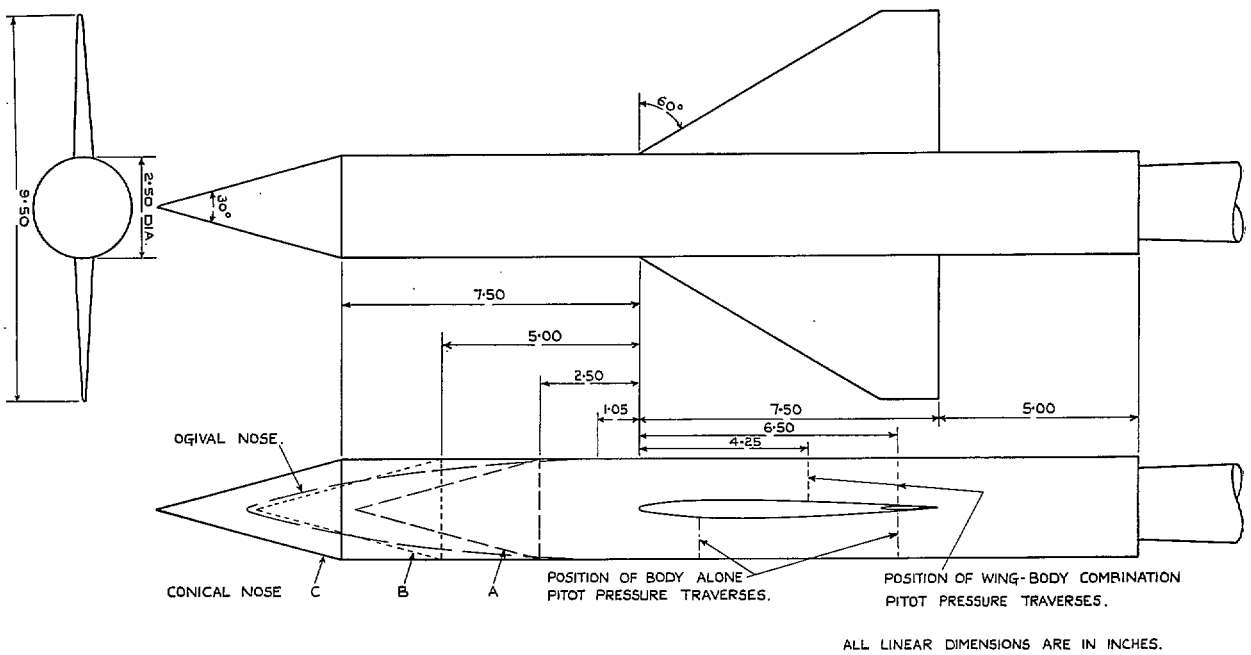

FIG. 1. General arrangement of the delta-wing and body combination.

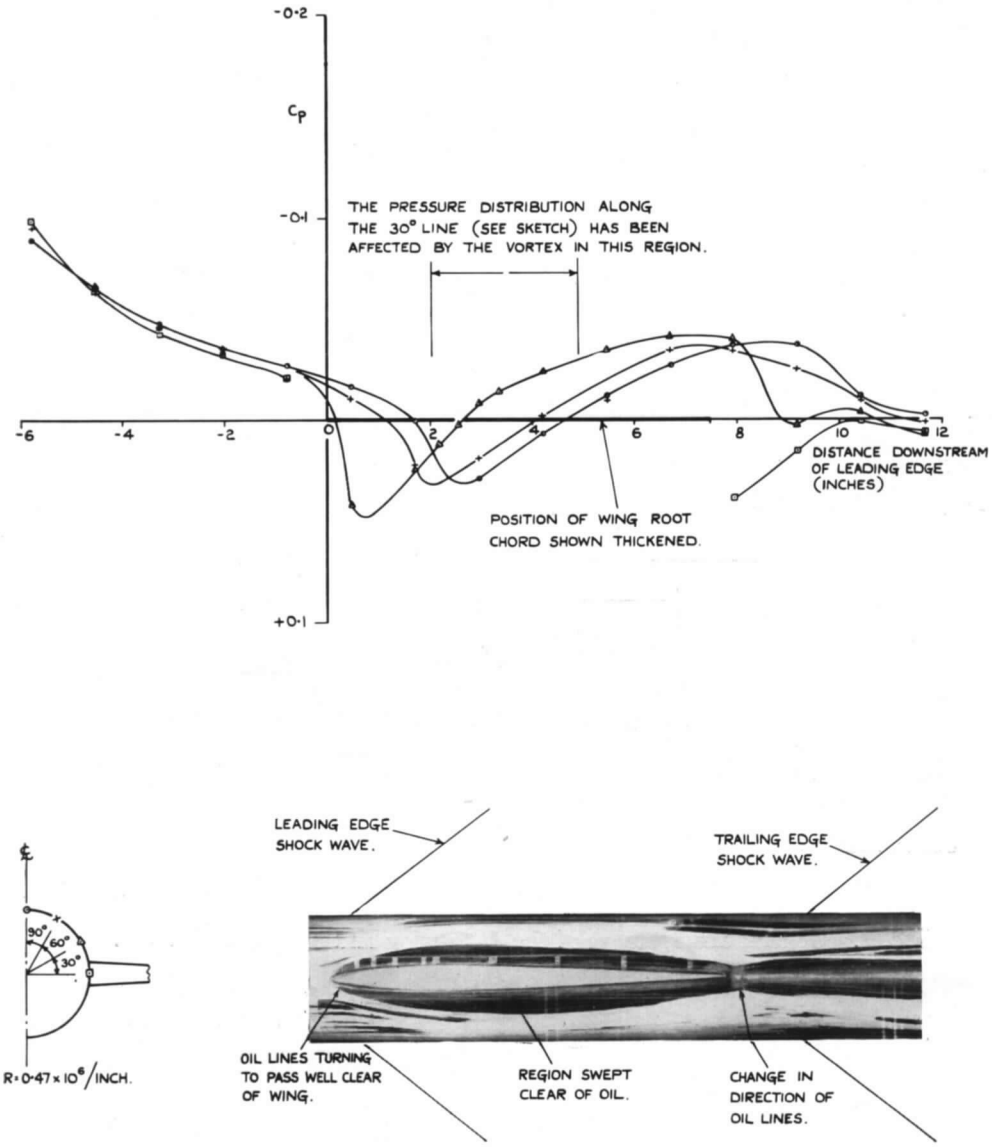

FIG. 2. Pressure distribution along the body and streamlines at the surface on the delta-wing and body combination at $M = 1{\cdot}61$ and $\alpha = 0$.

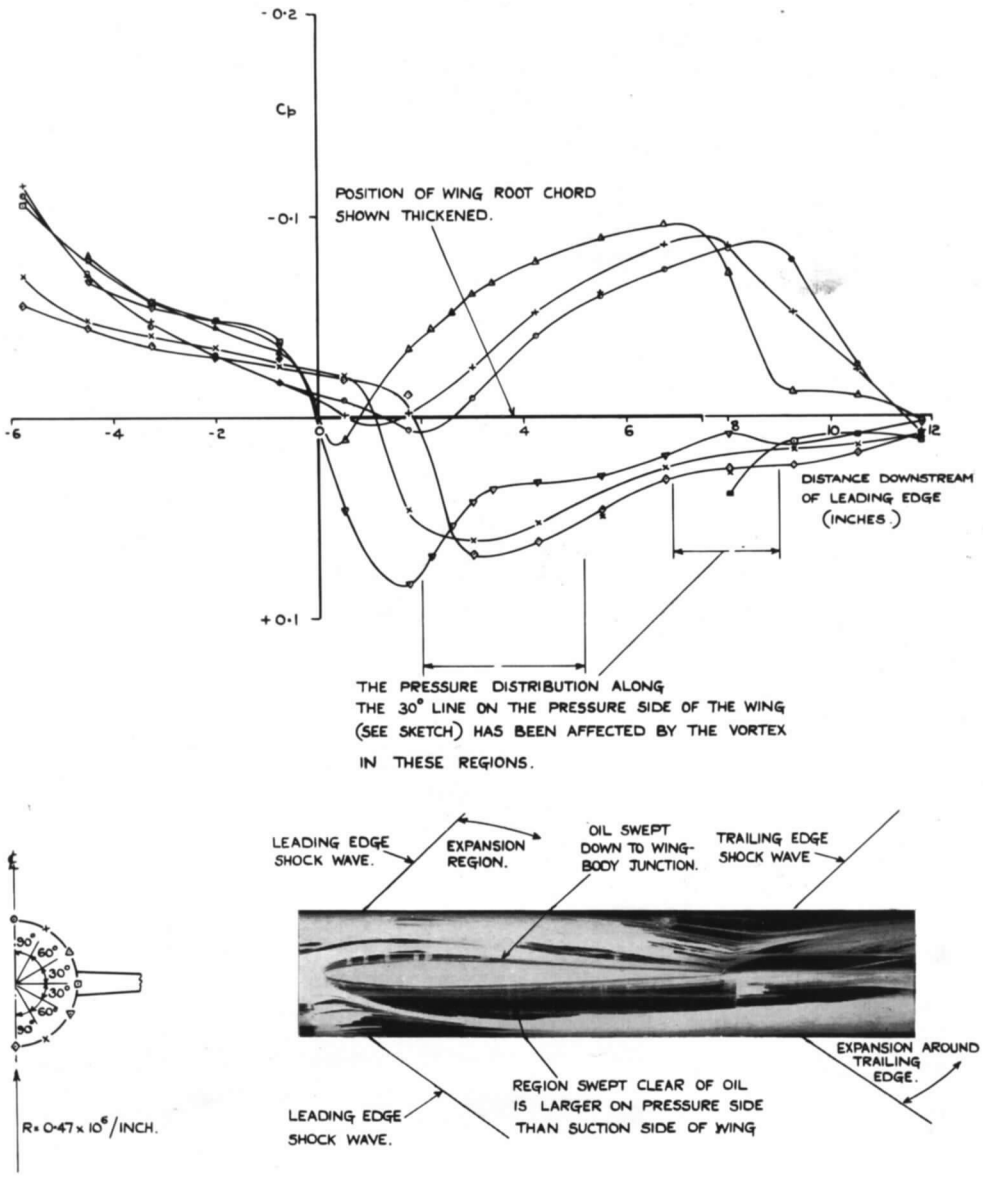

FIG. 3. Pressure distribution along the body and streamlines at the surface on the delta-wing and body combination at $M = 1{\cdot}61$ and $\alpha = 4$ deg.

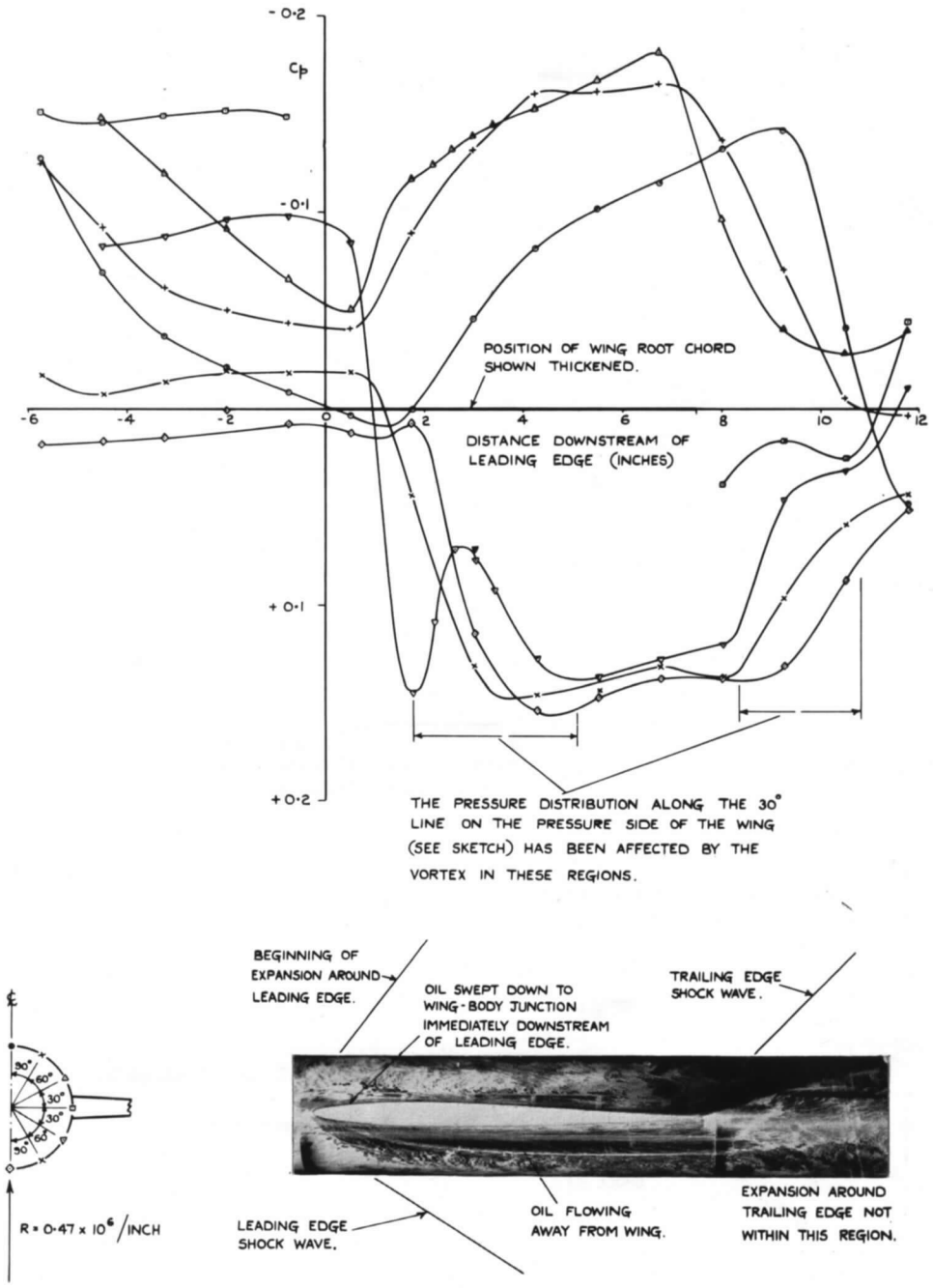

FIG. 4. Pressure distribution along the body and streamlines at the surface on the delta-wing and body combination at $M = 1{\cdot}61$ and $\alpha = 10$ deg.

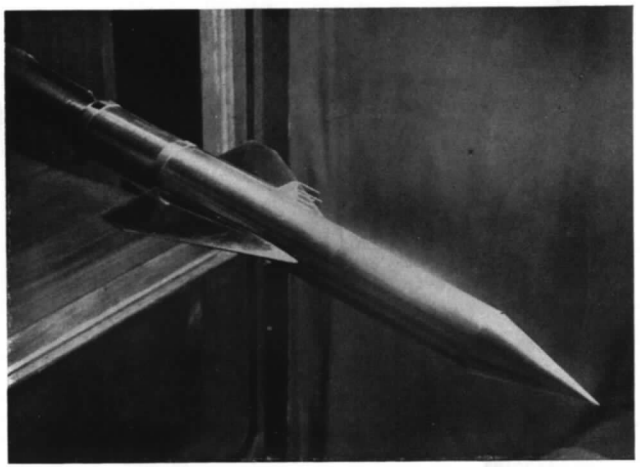

FIG. 5. The pitot-tubes in position on the body.

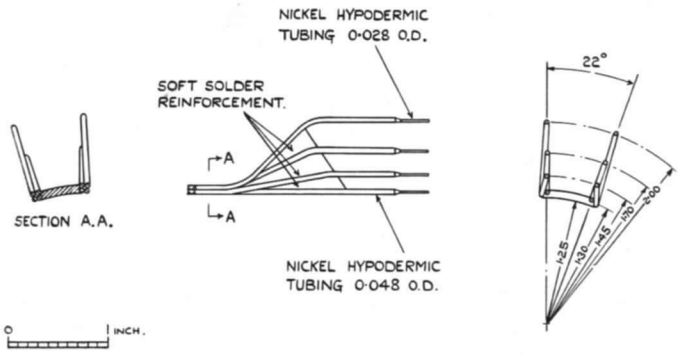

FIG. 6. Details of the pitot-pressure probes.

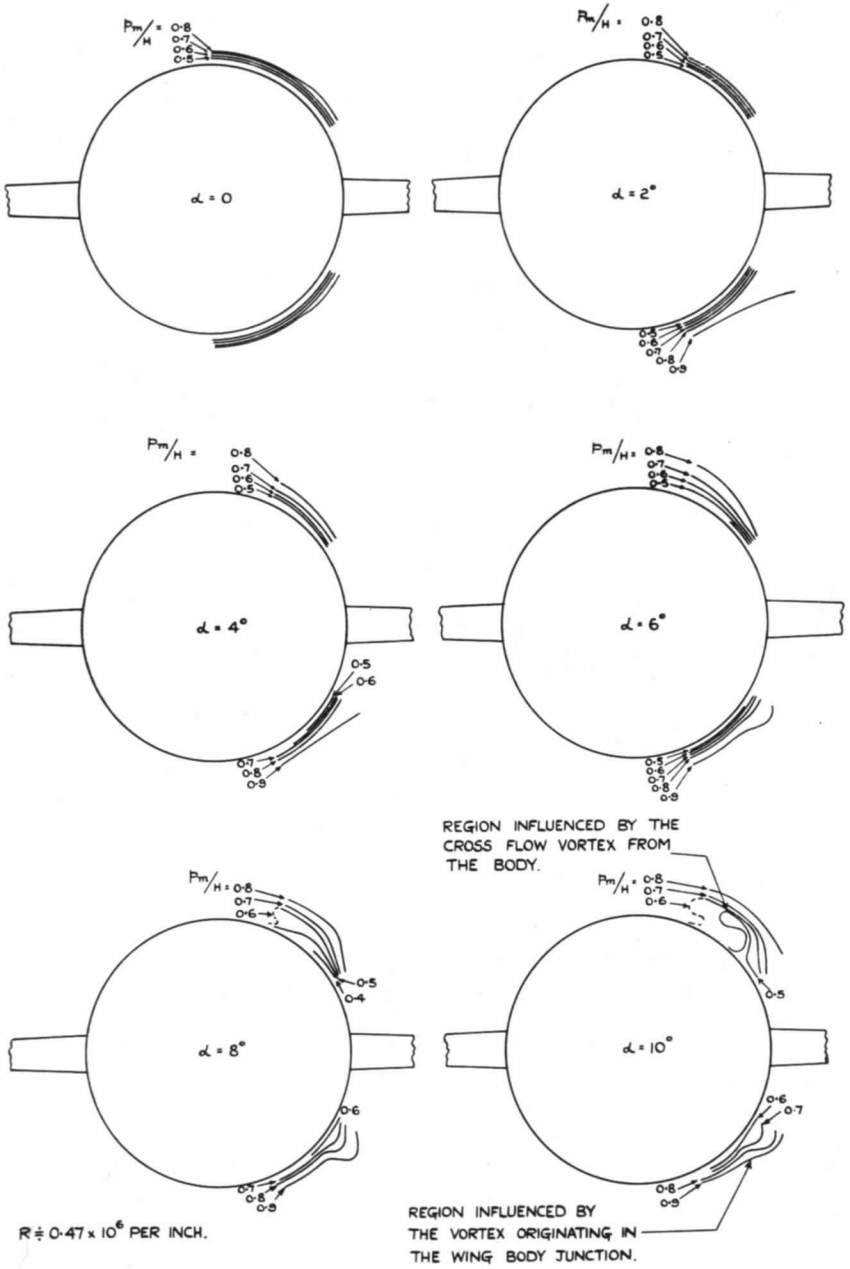

FIG. 7. Contours of p_m/H at 0·57 root chord. Delta-wing and body combination with nose C at $M = 1{\cdot}61$.

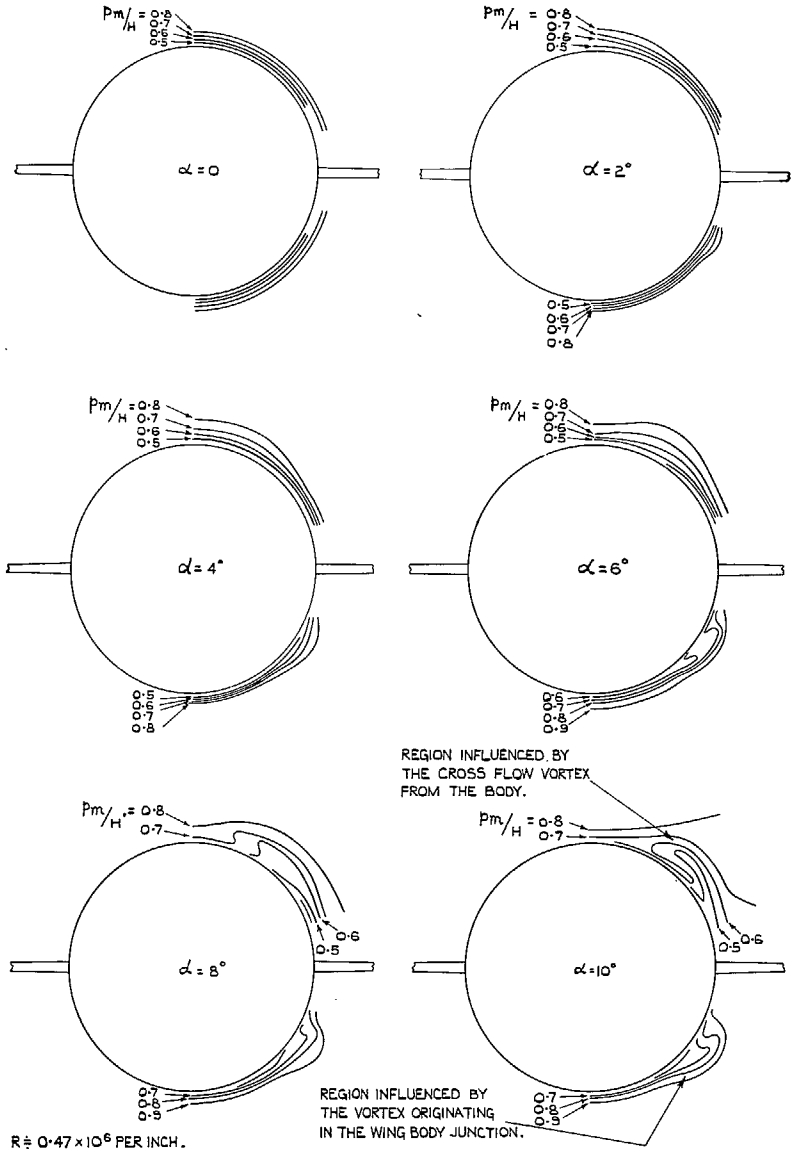

FIG. 8. Contours of p_m/H at 0·87 root chord. Delta-wing and body combination with nose C at $M = 1{\cdot}61$.

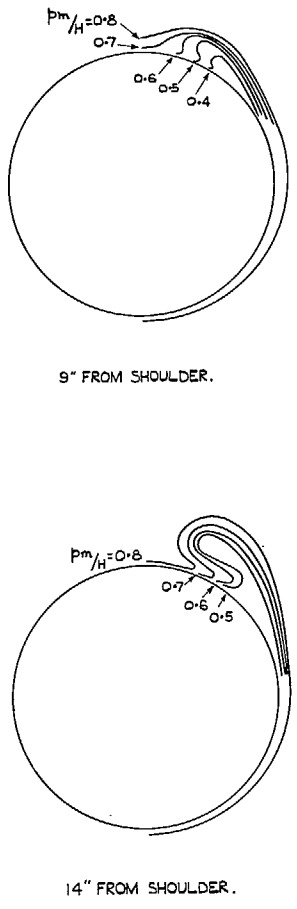

FIG. 9. Contours of p_m/H around the conical-nosed body alone at $M = 1{\cdot}61$ and $\alpha = 10$ deg.

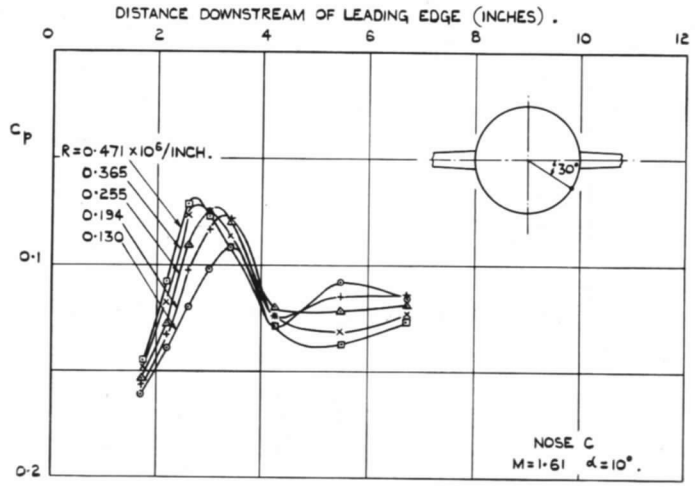

FIG. 10. The effect of varying Reynolds number on the surface streamlines and on the pressure distribution along the body in the presence of the delta wing.

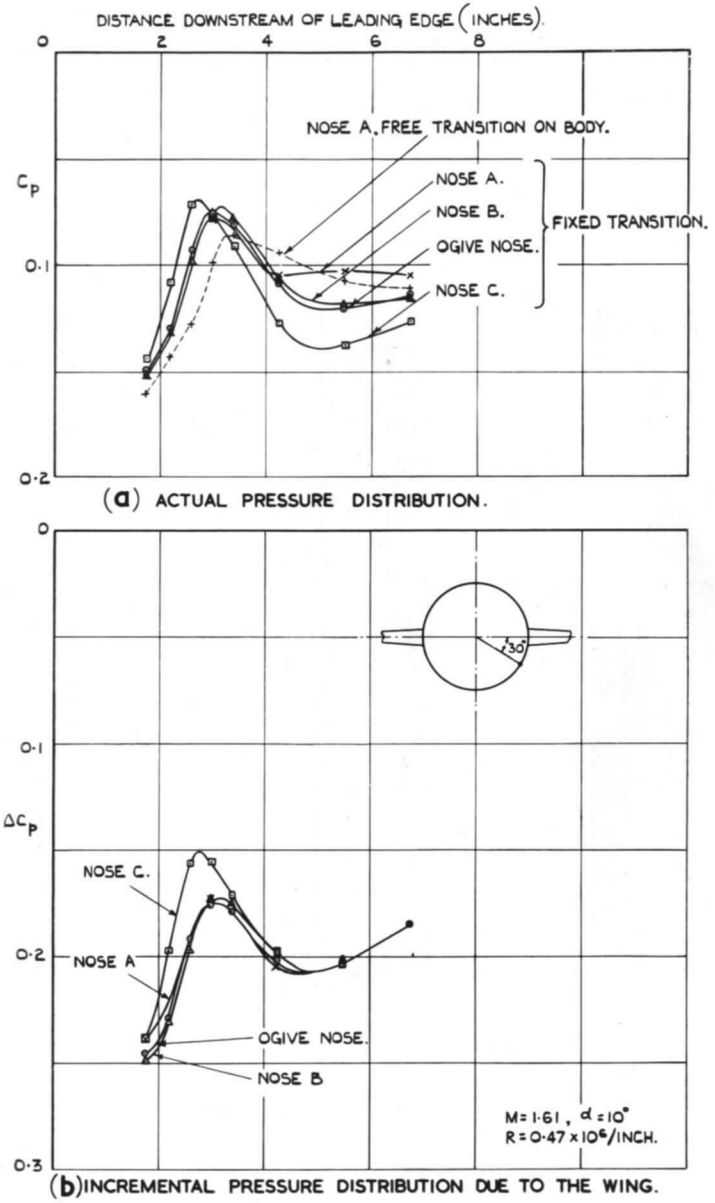

FIGS. 11a and 11b. The effect of varying nose length on the pressure distribution along the body in the presence of the delta wing.

a. $\alpha = 0°$

b. $\alpha = 4°$

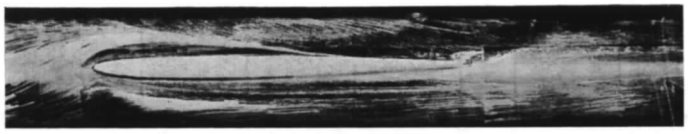

c. $\alpha = 10°$ R = 0.47 X 10^6/ inch

FIGS. 12a to 12c. Streamlines at the body surface in the presence of the delta wing at $M = 0{\cdot}70$.

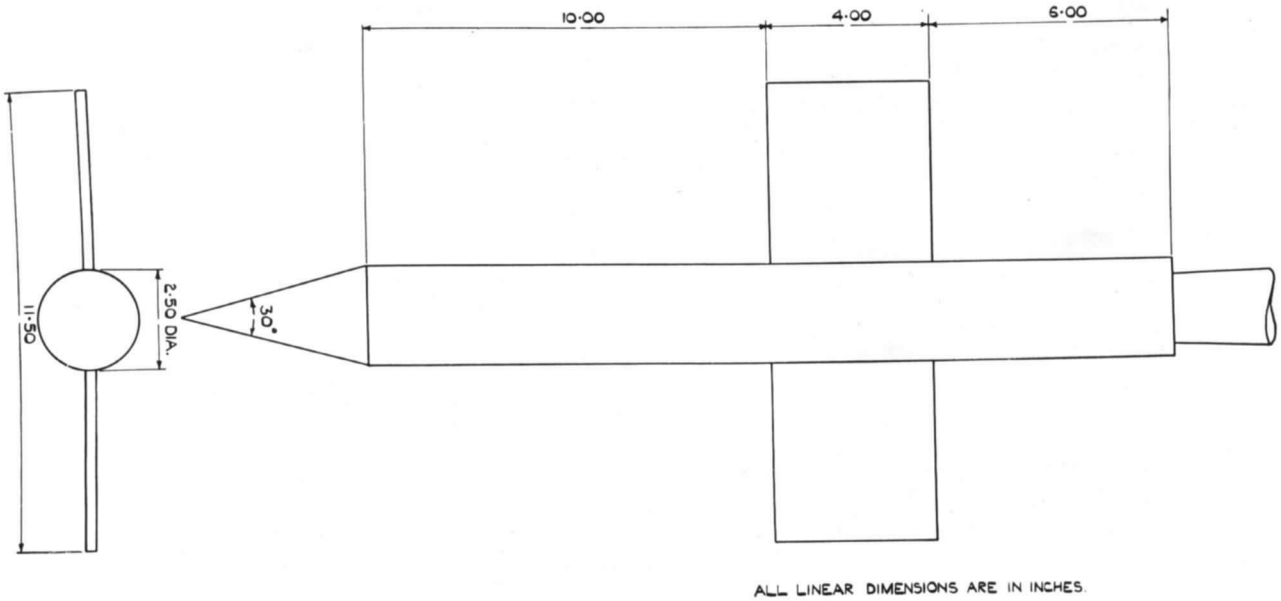

FIG. 13. General arrangement of the rectangular-wing and body combinations.

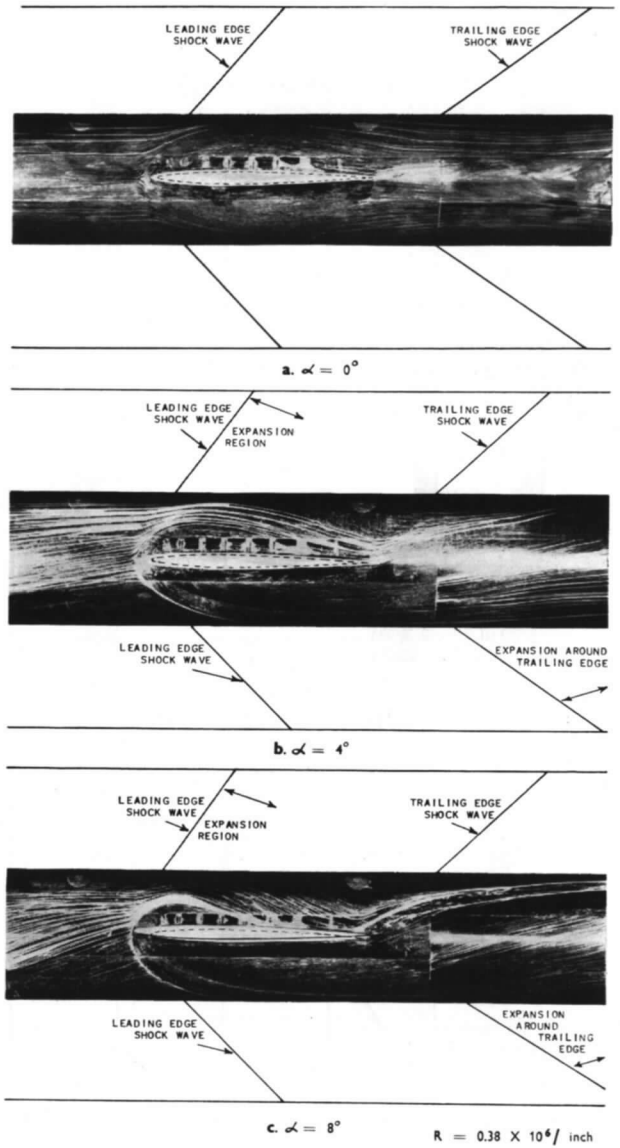

FIGS. 14a to 14c. Streamlines at the body surface in the presence of the rectangular wing (RAE 101 section) at $M = 1{\cdot}61$.

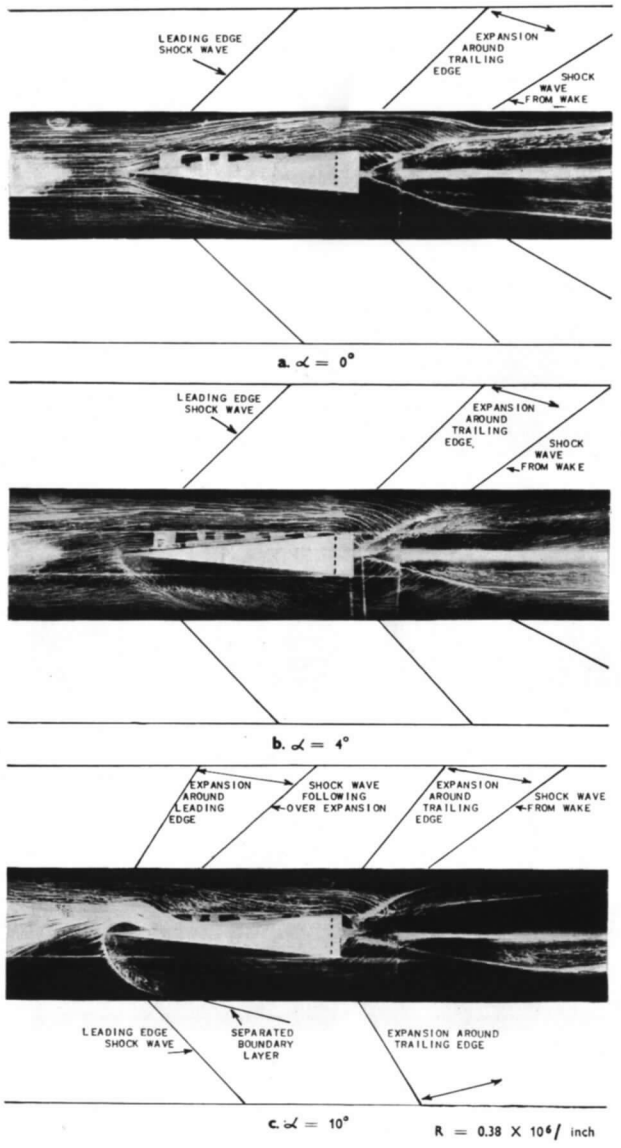

FIGS. 15a to 15c. Streamlines at the body surface in the presence of the rectangular wing (Wedge section) at $M = 1{\cdot}61$.

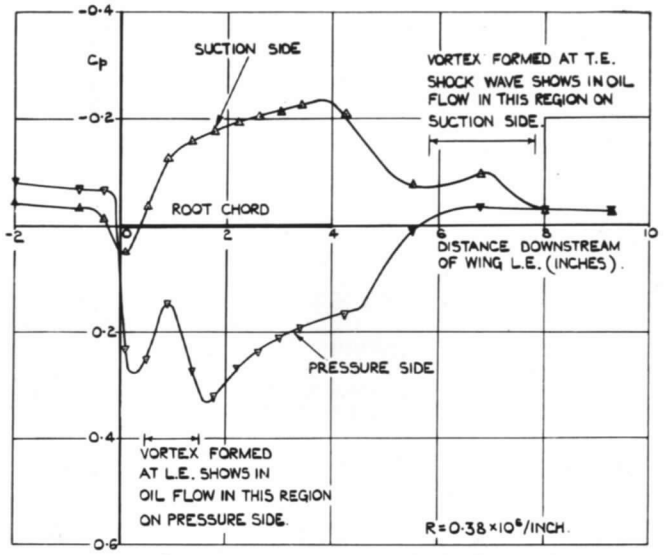

(a) R.A.E.101 SECTION, $\alpha = 8°$.

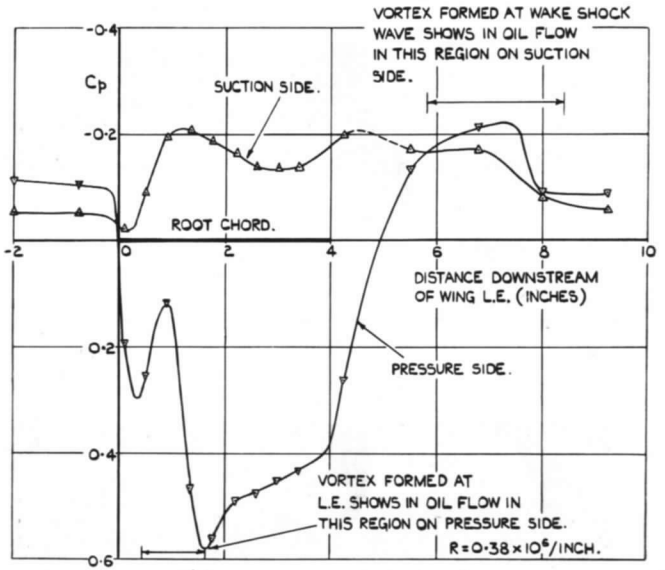

(b) WEDGE SECTION, $\alpha = 10°$.

FIGS. 16a and 16b. Pressure distribution along the body 30 deg from plane of wing in the presence of the rectangular wings at $M = 1{\cdot}61$.

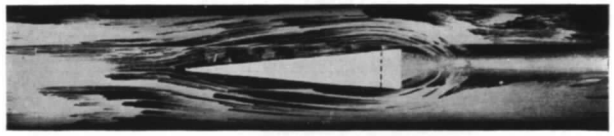

a. WEDGE SECTION $\alpha = 0°$

b. R.A.E. 101 SECTION $\alpha = 0°$

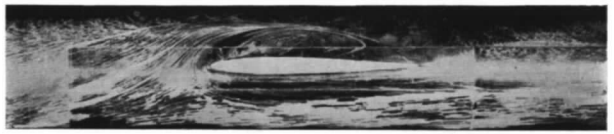

c. R.A.E. 101 SECTION $\alpha = 8°$

R = 0.38 X 10^6/ inch

FIGS. 17a to 17c. Streamlines at the body surface in the presence of the rectangular wings at $M = 0{\cdot}70$.

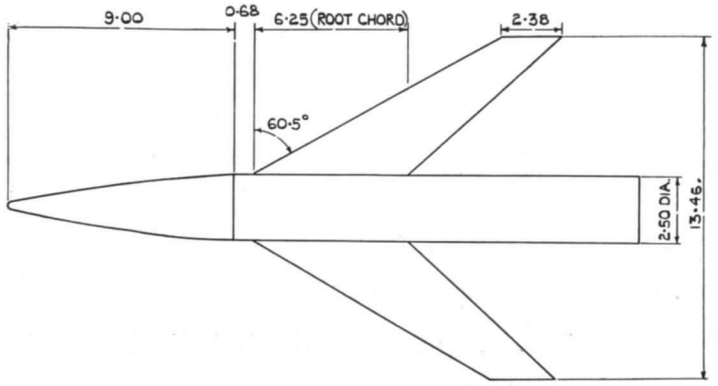

FIG. 18. General arrangement of the swept-wing and body combination.

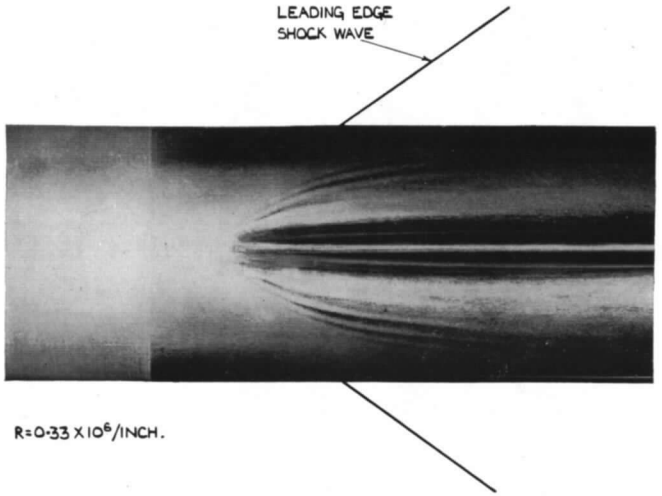

FIG. 19. The azobenzene pattern obtained at $M = 1{\cdot}81$, $\alpha = 0$.

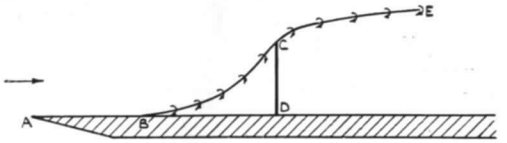

FIG. 20. The flow past a two-dimensional flat plate in a boundary layer.

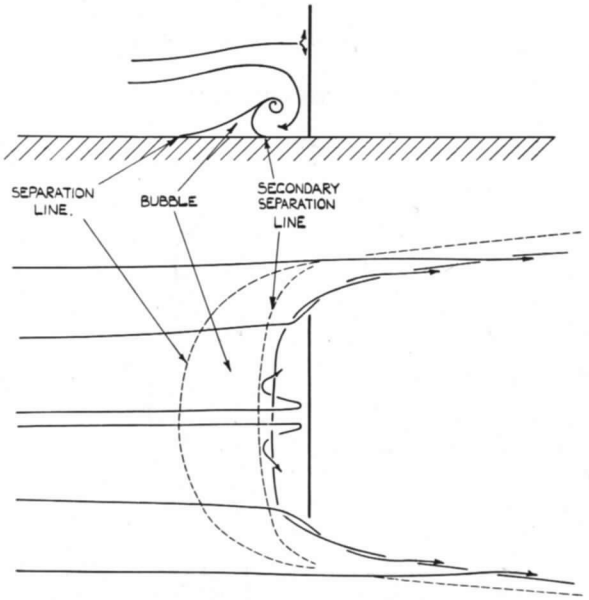

FIG. 21. The flow past a flat plate of finite span in a boundary layer.

(74881) Wt. 53/2293. K.7 8/59 Hw.

PRINTED IN GREAT BRITAIN

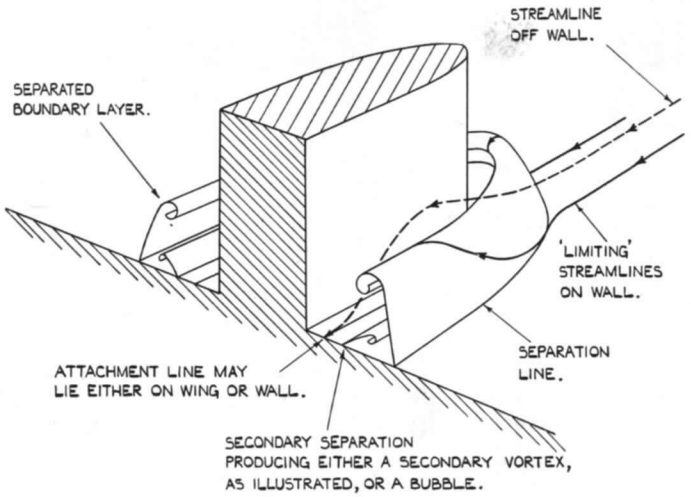

FIG. 22. The flow around a wing root.

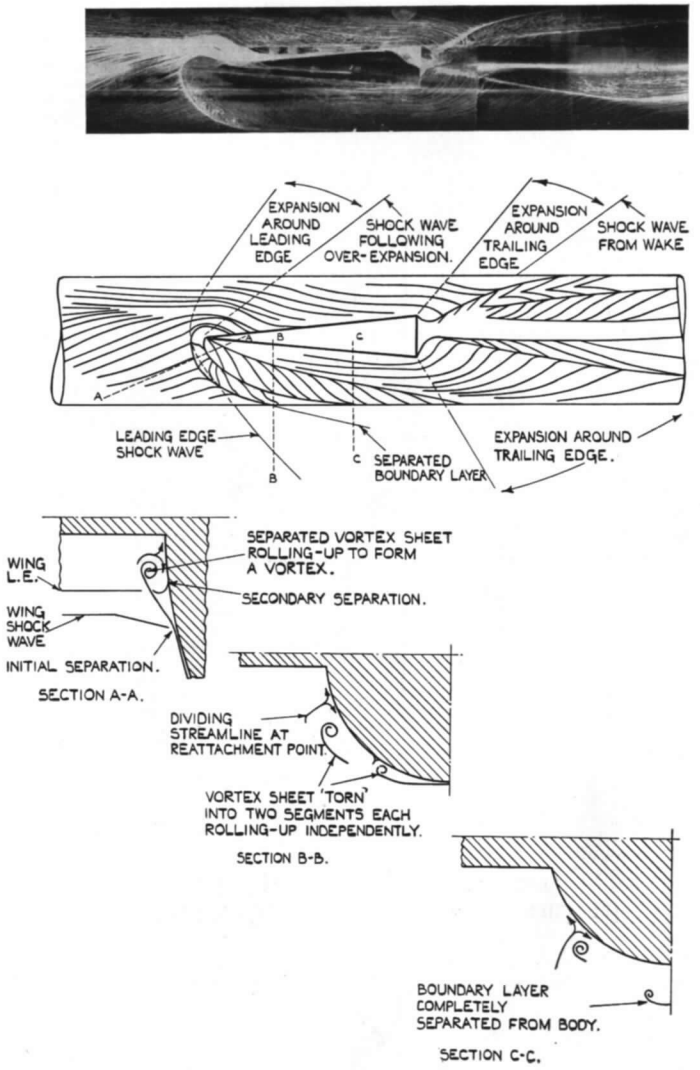

FIG. 23. A diagrammatic representation of the oil-flow pattern in FIG. 15c.

Publications of the Aeronautical Research Council

ANNUAL TECHNICAL REPORTS OF THE AERONAUTICAL RESEARCH COUNCIL (BOUND VOLUMES)

1939 Vol. I. Aerodynamics General, Performance, Airscrews, Engines. 50*s.* (52*s.*).
Vol. II. Stability and Control, Flutter and Vibration, Instruments, Structures, Seaplanes, etc. 63*s.* (65*s.*)

1940 Aero and Hydrodynamics, Aerofoils, Airscrews, Engines, Flutter, Icing, Stability and Control, Structures, and a miscellaneous section. 50*s.* (52*s.*)

1941 Aero and Hydrodynamics, Aerofoils, Airscrews, Engines, Flutter, Stability and Control, Structures. 63*s.* (65*s.*)

1942 Vol. I. Aero and Hydrodynamics, Aerofoils, Airscrews, Engines. 75*s.* (77*s.*)
Vol. II. Noise, Parachutes, Stability and Control, Structures, Vibration, Wind Tunnels. 47*s.* 6*d.* (49*s.* 6*d.*)

1943 Vol. I. Aerodynamics, Aerofoils, Airscrews. 80*s.* (82*s.*)
Vol. II. Engines, Flutter, Materials, Parachutes, Performance, Stability and Control, Structures. 90*s.* (92*s.* 9*d.*)

1944 Vol. I. Aero and Hydrodynamics, Aerofoils, Aircraft, Airscrews, Controls. 84*s.* (86*s.* 6*d.*)
Vol. II. Flutter and Vibration, Materials, Miscellaneous, Navigation, Parachutes, Performance, Plates and Panels, Stability, Structures, Test Equipment, Wind Tunnels. 84*s.* (86*s.* 6*d.*)

1945 Vol. I. Aero and Hydrodynamics, Aerofoils. 130*s.* (132*s.* 9*d.*)
Vol. II. Aircraft, Airscrews, Controls. 130*s.* (132*s.* 9*d.*)
Vol. III. Flutter and Vibration, Instruments, Miscellaneous, Parachutes, Plates and Panels, Propulsion. 130*s.* (132*s.* 6*d.*)
Vol. IV. Stability, Structures, Wind Tunnels, Wind Tunnel Technique. 130*s.* (132*s.* 6*d.*)

Annual Reports of the Aeronautical Research Council—

1937 2*s.* (2*s.* 2*d.*) 1938 1*s.* 6*d.* (1*s.* 8*d.*) 1939–48 3*s.* (3*s.* 5*d.*)

Index to all Reports and Memoranda published in the Annual Technical Reports, and separately—

April, 1950 - - - - R. & M. 2600 2*s.* 6*d.* (2*s.* 10*d.*)

Author Index to all Reports and Memoranda of the Aeronautical Research Council—

1909—January, 1954 R. & M. No. 2570 15*s.* (15*s.* 8*d.*)

Indexes to the Technical Reports of the Aeronautical Research Council—

December 1, 1936—June 30, 1939	R. & M. No. 1850	1*s.* 3*d.* (1*s.* 5*d.*)
July 1, 1939—June 30, 1945	R. & M. No. 1950	1*s.* (1*s.* 2*d.*)
July 1, 1945—June 30, 1946	R. & M. No. 2050	1*s.* (1*s.* 2*d.*)
July 1, 1946—December 31, 1946	R. & M. No. 2150	1*s.* 3*d.* (1*s.* 5*d.*)
January 1, 1947—June 30, 1947	R. & M. No. 2250	1*s.* 3*d.* (1*s.* 5*d.*)

Published Reports and Memoranda of the Aeronautical Research Council—

Between Nos. 2251–2349	R. & M. No. 2350	1*s.* 9*d.* (1*s.* 11*d.*)
Between Nos. 2351–2449	R. & M. No. 2450	2*s.* (2*s.* 2*d.*)
Between Nos. 2451–2549	R. & M. No. 2550	2*s.* 6*d.* (2*s.* 10*d.*)
Between Nos. 2551–2649	R. & M. No. 2650	2*s.* 6*d.* (2*s.* 10*d.*)
Between Nos. 2651–2749	R. & M. No. 2750	2*s.* 6*d.* (2*s.* 10*d.*)

Prices in brackets include postage

HER MAJESTY'S STATIONERY OFFICE

York House, Kingsway, London W.C.2; 423 Oxford Street, London W.1; 13a Castle Street, Edinburgh 2; 39 King Street, Manchester 2; 2 Edmund Street, Birmingham 3; 109 St. Mary Street, Cardiff; Tower Lane, Bristol 1; 80 Chichester Street, Belfast, *or through any bookseller.*

S.O. Code No. 23-3114